國 立 交 通 大 學

生物科技系所

碩 士 論 文

建立於奈米線場效電晶體上的高靈敏度、無須標記且即時偵測的腸病毒 DNA 生物感測器

Poly crystalline silicon nanowire field effect transistor based biosensor for highly sensitive, label-free and real-time detection of enterovirus DNA

研究生 ：賴文燦

指導教授 ：楊裕雄 教授

中 華 民 國 九 十 九 年 七 月

建立於奈米線場效電晶體上的高靈敏度、無須標記且即時偵測的腸病毒 DNA 生物感測器

Poly crystalline silicon nanowire field effect transistor based biosensor for highly sensitive, label-free and real-time detection of enterovirus DNA

研 究 生：賴文燦　　Student：Wen-Tsan Lai

指導教授：楊裕雄　　Advisor：Yuh-Shyong Yang

國 立 交 通 大 學

生 物 科 技 系 所

碩 士 論 文

A Thesis

Submitted to Department of Biological Science and Technology

College of Biological Science and Technology

National Chiao Tung University

in partial Fulfillment of the Requirements

for the Degree of

Master

in

Biological Science and Technology

July 2010

Hsinchu, Taiwan, Republic of China

中華民國九十九年七月

建立於奈米線場效電晶體上的高靈敏度、無須標記且即時偵測的腸病毒 DNA 生物感測器

學生：賴文燦　　指導教授：楊裕雄　教授

國立交通大學生物科技系所 碩士班

摘要

腸病毒七十一型(Enterovirus 71)對世界各地的幼童而言是一種重要的致病原且比其他非小兒麻痺腸病毒具有高致病率及致死率，其感染屬於神經性症狀,受感染的病童平均會在三天內惡化成重症。過去的臨床確認檢驗方式需要先作病毒培養再進行病毒分離和藉由反轉錄聚合酶鏈鎖反應(RT-PCR)，這些檢驗流程趕不上惡化成重症的時間，無法達到即時診斷出 EV 71 並作後續的醫療處置和疾病控管。在過去的文獻中，多晶矽奈米線場效電晶體可被製成且具有高靈敏度、無需標誌且即時偵測生物分子的生化感測器。將特定腸病毒的 DNA 序列有專一性的單股DNA序列先固定在多晶矽奈米線場效電晶體表面，將互補和非互補的 DNA 序列流過奈米線場效電晶體表面，能對 DNA 序列作專一性辨識而兩互補的 DNA 序列產生雜交反應使奈米線場效電晶體的導電度產生變化,最低 濃度可偵測到 fM (femto-molar, 10^{-15}M)。

此結果表示多晶矽奈米線場線電晶體具有高靈敏度、無需標誌且可即時偵測的潛能，此特性可發展成生物感測系統用來偵測腸病毒的感染型別並應用於其他傳染病篩檢。

Poly crystalline silicon nanowire field effect transistor based biosensor for highly sensitive, label-free and real-time detection of enterovirus DNA

Student: Wen-Tsan Lai Advisor: Yuh-Shyong Yang

Department of Biological Science and Technology, National Chiao Tung University

ABSTRACT

Enterovirus 71 (EV 71) is an important pathogen that causes higher morbidity and mortality in children around the world than those of other non-Polio enteroviruses. Its infection is neurotropic and even followed by rapid deterioration within average 3 days. The standard clinical methods for EV 71 identification require virus isolation in cell culture and reverse transcriptase polymerase chain reactions (RT-PCR). Virus isolation requires 5-10 days and hinders the subsequent treatment and disease control. Poly silicon nanowire field effect transistor has been shown to function as transducer for high sensitive, label-free and real-time biosensing to detect enterovirus infection. The selectivity of target for detection can be achieved by surface modification on NWFET. In our research, specific antibody or DNA sequences that recognize capsid protein or nucleic acid will be immobilized on poly Si NWFET. Currently, we are able to distinguish between EV 71 and CA 16 DNAs by real-time electrical analysis. It will be a promising biosensor for rapid diagnosis of EV 71 or other epidemic diseases.

Acknowledgement

自研究所進入LEPE 實驗室以來已經兩個年頭了，從當初懵懵懂懂的新生到現在已經是要畢業的學長，這經過的時間說穿了也不過是兩年，但其中經歷過的心歷路程可能遠超過以往的學生生涯。面對過不少問題與挫折，也在面對問題的過程中學習如何解決問題的態度，也遇到了許多幫助我解決問題的良師益友們。首先是感謝我的指導教授楊裕雄教授提供了一個風氣自由的研究環境，我在這裡能夠培養解決問題的能力並且藉由跟實驗室的同仁們討論，從各種角度去探討跨領域研究的問題點。這當中少不了實驗室成員們的幫忙，從一開始帶我跑元件製程的若芬學姊和陪我爆肝的戰友康寧；提出很多想法和見解給我思考的程允學長；對實驗要求很嚴謹的政哲學長；帶我做ELISA的小米學姊；幫我推拿整骨的淵仁學長；傳授許多實驗訣竅和投影片整理技巧的小志、秀華和音汝；做任何事總是面面俱到的陸宜；很熱心卻很跳tone的小胖；酒量驚人的普普、咏馨、晨竹還有欣怡，經過各位的薰陶之下，我的酒量確實有明顯進步；還有實驗室陸陸續續進來的新生也為實驗室注入一股新的活力；特別感謝NDL跟我們合作的明霈學長，明天要上班卻陪我們做實驗做到三更半夜。最後，我由衷地感謝長久以來默默支持我讀書的父母，你們的支持就是對我最大的鼓勵，這份感恩之情難以言喻。感謝能夠有緣份和各式各樣的人接觸學習造就了今天的我。

賴文燦　民國九十九年　八月

Contents

Contents of Tables

Contents of Figures

Abbreviations

NWFET: Nanowire Field Effect Transistor

APTES: 3-Aminopropyltriethoxysilane

EV 71: Enterovirus 71

CA 16: Coxsackie Virus A 16

fM: femto-molecular (10^{-15} M)

PDMS: Polydimethylsiloxane

I. Introduction

1.1 *Enterovirus*

1-1.1 *Introduction of Enterovirus*

The enterovirus belongs to family Picornaviridae, single-strand RNA virus. They consist of poliovirus (PV, 1-3 serotypes), coxsackie virus group A (CA, 1-22, 24 serotypes), group B (CB, 1-6 serotypes), and echo virus (EV, 1-33 serotypes, except 8, 10, 28) [1]. Since the 1960s, 4 newer enteroviruses have been discovered and named with serial number only, such as enterovirus 68-71 [2, 3]. After 2000, enteroviruses were classified by genomic sequencing to human poliovirus and human enteroviruses A to D [4] (Table 1). The major outbreak occurred in Taiwan is Enterovirus 71 in the summer of 1998 [5].

Enterovirus 71 (EV 71) belongs to human enterovirus A (HEV-A). EV 71 was further classified by their nucleotide sequence to genotype A, B, and C. Genotype B could be further classified into subtypes B1 to B5; and genotypes C into subtypes C1 to C5 [6, 7]. EV 71 and coxsackie virus A16 (CA 16) are both cause hand-foot-mouth disease (HFMD), but EV71 associated with the further development of acute neurological disease, including poliomyelitis-like paralysis, encephalitis, and aseptic meningitis. The primary agent in fatal case was EV71 which defined by the endemic in Taiwan in 1998 [3].

1-1.2 *Transmission Pathway*

EV71 is primarily transmitted through the fecal-oral route. Respiratory droplets are another route of transmission. Enteroviruses have been detected in water, soil, vegetables and shellfish and may possibly be transmitted in the community by contact with contaminated food or water. According to Chang's research during the 1998 epidemic, the isolation rate of throat swabs was higher than rectal swabs. EV71 could survive 1-2 weeks in the pharynx and 6-8 weeks in feces. It suggested that during the acute phase of disease, the respiratory droplets or saliva of patients are highly contagious and indicates that in limiting the spread of the epidemic, the respiratory isolation of HFMD patients could be important [8]. It's difficult to distinguish the specific cause of most enterovirus infection in clinical screening. Most enterovirus infection usually develops no clinical symptoms, mild upper respiratory symptoms, a flu-like illness with fever, or self-limited infections, like Hand-foot-and-mouth disease (HFMD) and herpangina(Table 2). But some may develop severe neurologic disease or die, especially in young children[3] (Table 3). After the incubation period ranges from 2-10 days, usual duration of illness is 3~6 days, symptoms start with fever and general malaise[9]. After morbidity, its rapid deterioration average within 3 days, and the majority of EV71 infected with severe complications are myoclonic jerks, hyperglycemia, encephalomyelitis and cardiopulmonary failure…etc [3, 5, 10].

1-1.3 *Epidemiology*

Young children are most susceptible to EV infection. Males more often develop clinically-recognizable disease than females[12]. Enterovirus 71 was first isolated from the stool of an infant with aseptic meningitis in California of the United States in 1969 [13]. Since then, EV 71 has been identified in many parts of the world. Two patterns of EV 71 outbreak have been classified. Small outbreaks involve with occasional patient death, this occurred in the United States, Australia, Sweden, and Japan [14-17]. The other severe outbreaks associated with high mortality, which occurred in Bulgaria in 1975 with 44 deaths [18], in Hungary in 1978 with 45 deaths [19], in Malaysia with at least 30 deaths [20], and in Taiwan in 1998 with 78 deaths [21], in 2000 with 25 deaths, in 2001 with 26 deaths [3]. Outbreaks of aseptic meningitis associated with enterovirus infection have been reported from Cyprus in 1996 and Gaza strip in 1997 [22]. The historical perspective and case incidences worldwide [3, 18, 19] are shown as Table 4 and Figure 1. To catalog of the incidence and case-fatality rate of enterovirus infections from 1998 to 2008 in Taiwan was shown in Figure 2.

1-1.4 *Current clinical diagnosis methods*

The traditional “gold standard” for the diagnosis of Enterovirus infection is virus isolation from clinical specimens in cell culture, following serotype identification by

neutralization test (NT) and detection of specific enterovirus serotype by the indirect immunofluorescence assay (IFA) [23-25]. The final identification was carried out using a number of different molecular approaches, including reverse transcription polymerase chain reaction (RT-PCR), restriction fragment length polymorphism (RFLP) analysis, and nucleotide sequence analysis of amplicons from various regions of the genome[23, 25-27]. There are some classified principles from CDC in this thesis.

1-1.4.1 *Enterovirus isolation in cell culture*

Diagnosis is made by detecting virus in throat or fecal swab samples, or more convincingly, from specimens collected of the affected part of the body, for example, cerebrospinal fluid (CSF), biopsy material, and skin lesions. A monkey cell line (LLC-MK2), human lung cell line (MRC-5), human rhabdomyosarcoma cell line (RD), African green monkey kidney cell line (Vero), human lung carcinoma cell line (A549), and human epidermoid carcinoma cell line (Hep-2) were used to grow viruses [23, 25]. Preliminary identification is based on the appearance of a minimum of 14 days for characteristic of a viral cytopathic effect (CPE)[28, 29].

1-1.4.2 *Enterovirus antisera neutralization test (NT)*

Serotype identification was performed by neutralization using Lim Benyesh-Melnick (LBM) pools of types-specific antisera. The serum specimen was

diluted by PBS, mixed well, and the mixtures were heated. Then the method of gold standard procedure was followed to make a two-fold serial dilution out of the sample, and a definite amount (100 $CCID_{50}$ / 50 μl) of virus was added to each of diluted solutions. The mixture was then incubated 4 days before its neutralization antibody titer determined [25, 30, 31]. At least, a four-fold rise in the level of neutralization antibody titer in serum collected during the acute and convalescent phase of illness, which provides the best evidence of a recent infection[2].

1-1.4.3 *Immunofluorescence assay (IFA)*

When cytopathic effect was observed, infected cells were scraped off the vessels, washed in PBS, spotted on the slides. The monoclonal antibody blends were directly applied to specific wells on each slide. The slides were incubated with a prestandardized dilution of anti-mouse immunoglobulin G fluorescence-conjugated antibody. After mounting, slides were then examined under a fluorescence microscope [23-25]. In Rigonan's research, the sensitivity of the IFA was 73% for polioviruses, 85% for coxsackieviruses type B, and 94% for echoviruses. Specificity was near 100% for polioviruses and coxsackieviruses type B and 94% for echoviruses[24].

1-1.4.4 *Reverse transcription polymerase chain reaction (RT-PCR)*

After RNA extraction, the purity and concentration of RNA was determined both measuring OD at A260/280 and by quantitating the ethidium-stained agarose gel

bands. RT-PCR were carried out by RT-PCR beads. The beads contained recombinant Moloney Murine Leukemia virus (M-MuLV) reverse transcriptase for cDNA synthesis, Taq DNA polymerase for amplification, RNase inhibitor, buffer, dNTPs. RT-PCR products were examined by electrophoresis through 1~ 3% agarose gels and ethidium bromide staining. The bands migrating at the predicted size were excised and purified for further sequencing analysis [23, 25, 32].

1-2 *Applying poly crystalline silicon nanowire field-effect transistor*

Conventional techniques for the detection of biomolecular interactions are limited by the need for exogenous labels, time- and labor-intensive protocols, as well as by poor sensitivity performance levels[35]. Material scientists and engineers have progressively miniaturized the materials with advanced CMOS fabrication process that constitute the building blocks of various biomedical devices, such as carbon nanotubes[43], surface plasma resonances (SPR)[44], cantilever[45], quartz crystal microbalance (QCM)[46], and quantum dots[47]. Some of these sensing devices, such as those based on cantilevers and quantum dots, are highly specific, ultrasensitive, and have a short response. However, these devices require integration with optical components transducing surface phenomena to collectable signals. The requirement for detection optics is expected to significantly increase the cost of operation for such a device. This progressive downscaling has led to the creation of materials with one

critical dimension less than the scale of approximately 100 nm at least. Table 5 compared the relative methods of biosensing, NW-FET can be developed to a highly sensitive, label-free, and real-time biosensor. In the present method, NW-FET has the highest sensitivity, and many research teams consider it as an important study direction.

II. Materials and Methods

2-1 *Experimental material*

1. 3-Aminopropyltriethoxysilane (APTES): $H_2N(CH_2)3Si(OC_2H_5)_3$

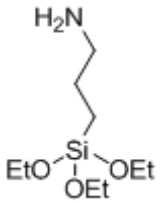

Company: Sigma-Aldrich (USA) (A3648)

CAS Number : 919-30-2

Assay: ≥98%

2. Sodium cyanoborohydride: $NaBH_3CN$

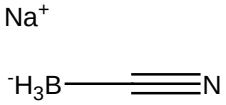

Company: Sigma-Aldrich (USA) (71435)

CAS Number : 25895-60-7

Assay: ≥95% (RT)

3. Ethanolamine hydrochloride: $NH_2CH_2CH_2OH \cdot HCl$

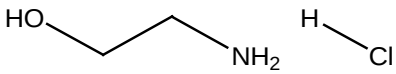

Company: Sigma-Aldrich (USA) (E6133)

CAS Number : 2002-24-6

Assay: ≥99%

4. Glutaraldehyde solution: $OHC(CH_2)_3CHO$

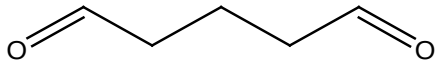

Company: Fluka (USA)

CAS Number : 111-30-8

Grade: technical

Concentration: ~25% in H_2O (2.6M)

5. Potassium phosphate monobasic: KH_2PO_4

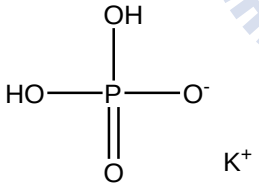

Company: J.T.Baker (USA)

6. potassium phosphate dibasic: K_2HPO_4

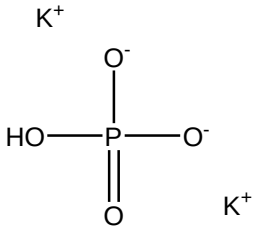

Company: J.T.Baker (USA)

7. Ethanol (99.5%): CH_3CH_2OH

Company: Echo Chemical Co. (Taiwain)

8. Polydimethylsiloxane (PDMS): $(H_3C)_3SiO[Si(CH_3)_2O]_nSi(CH_3)_3$

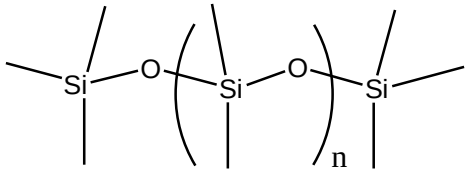

Company: Sil-More (Taiwan)

9. EV71 DNA sequences were designed for capture probe and the target DNA used on this project are listed as below and based on previous publication [27]. All synthetic oligonucleotides were purchased from MDBio Inc. (Taiwan).

5’-amino C_6 modified captured DNA probe

	DNA sequences (5’-3’)	
	5’-H_2N C_6 modified captured DNA probe	Target DNA
EV71 [a]	GTG GCA GAT GTG ATT GAG AG	CTC TCA ATC ACA TCT GCC AC
CA16 [b]	GAG TGA TGG TTC AAC ACA CA	TGT GTG TTG AAC CAT CAC TC

a relative to BrCr nt 2448-2467

b relative to G-10 nt 2666-2685

10. Phosphate buffer solution (PBS) was prepared by Potassium phosphate monobasic and Potassium phosphate dibasic dissolved in de-ionized

water at 10 mM, adjusting pH value by buffer titration.

11. Deionized water (DIW)

resistance of water: 18.2 MΩcm

ultra-pure water system (Barnstead).

2-2 *Instruments*

The whole instrument consisted of electrical measurement machine (Dual-channel System Source Meter Instrument Model 2636) (Keithley), probe station with its chamber (EVERBEING(奕葉)), and programming syringe pump (Kd Scientic) (Figure 4).

2-3 *Poly crystalline silicon NWFET fabrication process*

First, the fabrication began on Si wafers capped with a 100 nm-thick thermal oxide. The second, a 50nm-thick nitride layer was deposited by low-pressure chemical vapor deposition (LPCVD). After deposition of the nitride layer, following deposing Tetraethyl ortho-silicate (TEOS) 100nm thick sketched with standard photolithographic and etching steps were performed to form the oxide dummy structures. Subsequently, a 100nm-thick amorphous-Si layer was deposited and then annealed at 600°C for 24hr in N_2 ambient to transform it into polycrystalline structure. Afterwards, source/drain (S/D) doping was done with phosphorus ion implantation

with a dose of $5E^{15}cm^2$. After the generation of S/D photoresist patterns with a lithographic step, a reactive plasma etching step was performed to form the S/D regions. Because of the anisotropic etching process, two poly-Si NW channels were formed separating by oxide dummy gate simultaneously during the S/D etching step. By carefully controlling the etching time, the cross-sectional dimensions of poly-Si NW channels can be easily reduced to sub-10 nm scale. Subsequently, all devices were then covered with a 200nm-thick TEOS oxide passivation layer. Finally, remove the oxide layer by 2-step dry/wet etching process to expose the poly-Si NW channels.

2-4 *Microfluidic system*

The microfluidic channel system will be made with acrylic, PDMS and metal holder. First, the PDMS gel will be covered to the channel patterned glass substrate (channel size: 13 mm X 1 mm X 0.5 mm) at 120^{o}C for 10 minutes and wait for the fluid gel transfer to solid state. The solidification PDMS channel will be separated from the glass substrate and covered to the SNW chip. Then, make the limpid acrylic blanket and drill two holes filling with Teflon tubes (outer diameter: 1.5 mm, inner diameter: 0.5mm) for sample transport. Finally, limpid blanket of acrylic was covered to the PDMS and the chip-PDMS-acrylic sandwich was fastened by a metal holder. The advantage of the microfluidic channel system is easy alignment, easy observation

and be reused. The schematic diagram of the microfluidic system is shown in Figure 5.

2-5 *Surface modification*

We would do some treatments on chip surface before we measure the electrical variation. The immobilization process is based on the microfluidic system. Initially, we aligned the PDMS microfluidic channel covered on nanowire device row and added acrylic blanket on PDMS solid gel. Then, fastened the blanket and PDMS gel on nanowire chip by metal holder like the sandwich structure, tested whether the fluid buffer seep from the sandwich-stacking microfluidic system (Figure 5). After setting up the microfluidic system, it shall be locked an injection tubing connector. Inject APTES in ethanol solution 1 ml through microfluidic channel and react for 17~20 minutes. Then, wash the channel with 95% ethanol. Turn on hot plate and set the temperature about 110℃~120℃, put the whole microfluidic system on the hot plate for 10 minutes. Then, cool the metal holder to room temperature and inject 2.5% glutaraldehyde reacting for one and half hour in 10 mM pH 7 phosphate buffer. Nanowire surface functional group would be changed from hydroxide into aldehyde group, we would use DNA sequence modified amino-C6 at 5’ end as a DNA probe to bind with surface aldehyde. We Applied Yang’s research[27] to modify a 20-mer

DNA sequence diluted in 10mM pH 7 phosphate buffer, injecting 1 μM to microfluidic channel for 3 hours or more. Continuously, block unbinding aldehyde group with 50 mM ethanolamine at pH 9.1 phosphate buffer for one and half hour. Finally, wash the channel with pH 7 phosphate buffer and ready measure. The overall surface modification is shown in Figure 6.

2-6 *Sample transport at kinetic equilibrium*

In order to maintain the environment ionic strength level, we would keep the microfluidic channel fluent to replace of quiescent state. First, set the microfluidic system connecting a syringe pump at injection end and be locked a liquid gate at the elution end. The waste buffer shunted by T-shaped tubing (Figure 7), sealed the end of metal wire by silicone neutral sealant. Then, fix the flow velocity at 5 ml/h by Syringe Pump (Kd Science) (Figure 8). Sample will be exchanged by changing another syringe tube, a little bubble between two solution samples. The whole transport system is semi-automatic, which fixed flow velocity by machine but changed syringe tubes by people.

2-7 *Liquid phase electrical measurement*

It has been reported that the electrical properties would be different from air

to liquid phase environment. We would immobilize chemical compounds and biomaterials on nanowire chip in microfluidic channel for 6 hours, changed surface functional group in liquid phase. After treating the chip for a long time, we measured the device properties by conductance-time method, compared with those relations of the shift of threshold voltage to air condition and its' stability. We measured these data and calculated mathematically signal process, found the most sensitivity Vg point. We got a plot for describing the relationship of conductance-Vg (liquid gate) and a voltage which has the most sensitive variation rate. Then, fixed the Vg and measured pH sensing to check correcting variation trend.

III. Results and Discussion

3-1 *Nanowire chip selection in dry air condition*

Nanowire Field Effect Transistor (NWFET) wafers were fabricated at Class 100 clean room of National Nano Device Laboratory (Hsinchu city, Taiwan, R. O. C.), sealing in an anti-electrostatic bag. We need to check the electrical properties before biosensing, by using electrical analysis machine (Keithley 2636) to measure NWFET chips. For the purpose, one standard operation process was built (Figure 9) to screen good chips, record the data of Id-Vg plot and key parameters of threshold voltage, on/off current ratio (Figure 10-A& 10-B), and then, look for good and stable chips for biosensing. Chip selection principles were defined in Table 6, classified into three ranks, best, acceptable and failed.

3-2 *Biosensing of non-immobilized semiconductor device*

Initially, the control set of conductance measurement was calculated by measuring the electrical variation of bare chip. The real-time changeable conductance was observing in all experimental preparation setup. First, the microfluidic channel was filled with 10 mM pH 7 phosphate buffers and kept the buffer flowing. The conductance value won't change too much if we don't do any action. When the syringe tube was changed, a big pulse wave appeared, caused by the little bubble

between two buffer solutions. These results show it didn't change obviously because we just change the same solution to test whether the device is stable after the bubble pass through. Then, we injected 100 pM CA 16, the signal didn't change obviously after the bubble peak passed because of no immobilization on nanowire device. After CA 16 DNA sample was injected, washed the microfluidic channel by pH 7 buffer before next sample. Then, we switched EV 71 DNA sample, the signal still be kept in baseline. Finally, we washed the channel by pH 7 buffer solution to clean the microfluidic channel, the signal still be kept in baseline at last. Those overall results show that the conductance electrical signal won't change obviously without functionalizing nanowire device surface (Figure 11).

3-3 *Device characteristic verification in liquid phase*

After surface modification on NWFET chips, and the electrical characteristic of the device was tested. We want to know two main goals that the variation trend of the most sensitive voltage point is also based on the sensing theory. First, we swept the liquid gate voltage to check the electrical variation controlled by liquid and calculate these data. The conductance value (red line) (Figure 12) will be increased as liquid gate is increased and fitted the N-type device features. Then, differentiate the conductance value with liquid gate values to get G_m values. Finally, G_m values are

divided by conductance values (G) to get sensitivity values (Sensitivity=G_m / G , G_m = dG / dV). After those mathematic operations, we got the Vg value with maximum variation rate at sub-threshold region. Both biosensing and pH sensing shall be operated at fixed Vg value we calculated before. On the other side, we would check whether the variation trend of the conductance signals fitted its doping type. In this experiment, we applied N-type NWFET as sensing device, to observe the signal changeably fitting N-type characteristic. When the buffer switched from pH 7 to pH 8, it will have more negative ion than pH 7, to make N-type NWFET induced less electrons passing through those channels. Reversibly, buffer solution switched from pH 8 to pH 7, it has less negative ion than pH 8, to make N-type NWFET inducing more electrons pass through those channels. The conductance value is directly relative to the current of nanowire channels. As the results are shown in Figure 13, the conductance value could reversibly change from different pH buffers fitting N-type device characteristic.

3-4 *Enterovirus 71 (EV 71) DNA Biosensing*

After surface functional group modification and reaction with EV 71 DNA probes (Shown as Figure 6), we measured the real-time conductance signals of injecting buffer or samples in fixed flow rate by syringe pump (Kd Science). In the

experiment, the probe DNA was designed 20 base long and amino hexyl was modified at 5’-end with complementary DNA strand as target DNA but no modified at both ends.

In addition, we design a CA16 as a negative control to confirm the probe DNA of specifically binding to its’ complementary DNA. All samples were diluted by phosphate buffer (10 mM, pH 7.0) and we regard the buffer condition as baseline in the experiment. First, we would make a bubble to generate a signal pulse observing whether the baseline shift or not. So as to the other pulses when we switching to another samples, the bubble means to signal income. Second, it will be injected 10000 times concentration negative control (CA 16) than positive sample (EV 71) to observe whether the signal variation, then eluting the CA 16 with phosphate buffer. Third, inject the EV 71 1 fM into the channel to react with probe DNA. We can see those conductance value of 1 fM EV 71 obviously changed than 100 pM CA 16 as shown in Figure 14. Finally, we added 100 fM EV71 to check whether the reaction saturated, compared with those conductance changed percents among control and experiment data (Figure 15). As these results, the real-time conductance analysis method can specifically identify both complementary DNA and non-complementary DNA. The proposed measuring system has advantages like label-free, real-time and high sensitivity. It’s promising to develop semiconductor biosensor.

3-5 *EV 71 DNA biosensing after hot water washed*

After the EV 71 biosensing, we injected 10~15ml hot water (over 80 ℃) to remove the hybridized DNA sequence (T_m: 51.8 ℃). Then, washed the microfluidic channel by phosphate buffer (room temperature) and repeated previous process again. First, we would sweep liquid gate to observe the conductance value still controlled by liquid gate because we didn't know how the hot water affected the device characteristic. Secondly, got those data of conductance to liquid gate and calculate the most sensitivity Vg point. Compared to Figure 9, the most sensitive Vg point shifted to 1.65 V (Figure 16). We considered that (1) the device was decayed since the first biosensing process (2) after the hot water washed the device surface suffered damage. However, we followed up previous process to do biosensing again. In the beginning, the baseline was rised up continuously, even we injected CA 16 (control set) DNA sample. But the conductance value will be decreased obviously when EV 71 (experiment set) injected. We got the same response even though the baseline was not as flat as these previous results. We can say that the conductance signal could truly reflected bio-reaction on device surface (Figure 17).

3-6 *CA 16 DNA Biosensing*

In contrast to EV 71 biosensing, we do another experiment by immobilizing

CA16 DNA probe and detecting complementary CA 16 target sequence. The EV 71 DNA strand became control set in the experimental design. According to the same previous process to sweep the Vg, the most sensitive Vg point was calculated as shown in Figure 18. We got the Vg value about 1.03 V and started biosensing by the fixed Vg value. In the beginning of CA 16 biosensing, we injected 100 pM EV 71 DNA sample as control set, and the conductance value still be kept on baseline. Then, injected 1fM CA 16 and the conductance value didn't shift obviously. As injected 100 fM CA 16, the conductance value shifted down slowly. A little difference from EV 71 biosensing results, the conductance value would rise when we injected pH 7 PBS buffer to wash the channel. Similarly, we injected higher concentration of CA 16. It can obtain more variation than lower concentration samples, but still be recovered when buffer injected (Figure 19). After biosensing, we compared those different concentrations of CA 16 samples and control set (Figure 20), it was revealed the variation rate directly proportional to concentration. Finally, we proposed that the reason of the conductance value reversed when buffer injected. The distortion of microfluidic PDMS may change the streaming potential, to cause the hybridized DNA flushed by buffer. The higher concentration of CA 16 samples still be reacted with immobilized DNA probes. It still performed high specificity of biosensing because it didn't react with control set.

IV. Summary and perspective

In our research, we have demonstrated the poly crystalline silicon NWFET could be developed as a highly sensitive, specific and label-free biosensor to detect EV71 and CA16 nucleic acid in a real-time kinetic measurement system. The device yield is not yet as good as commercial products, we still provide a standard operation process to pick up good device for biosensing. By the lock-in detection and sample transport system, we could filter out a lot of noise to extract conductance signal. It helped us measuring bio-reaction at steady state. Not only apply on rapid diagnosis but also be suitable to investigate the molecular bio-reaction. Furthermore, the poly crystalline silicon NWFET fabrication process is compatible to modern semiconductor technology in Taiwan. It could be mass production for many applications. Therefore, the poly crystalline silicon NWFET could provide a great potential for real-time, label-free and highly sensitive molecular diagnostics or other scientific applications (Table 7).

V. Reference

1. 行政院衛生署疾病管制局. “*腸病毒感染併發重症(含非小兒麻痺病毒之腸病毒感染症)*”, 2007, [cited; Available from: http://www.cdc.gov.tw/index_info_info.asp?data_id=1007.
2. **Huang, K.Y. and Lin, T.Y. “*Enterovirus 71 infection and prevention*”, *Taiwan Epidemiology Bulletin*, 2008, p. 415-426**
3. **Lin T.Y. et al. “*The 1998 enterovirus 71 outbreak in Taiwan: Pathogenesis and management*”, *Clinical Infectious Diseases*, 2002, 34, p. S52-S57.**
4. **King, A.M. et al. “*Family Picornaviridae. In Virus Taxonomy.*, in *Seventh Report of the International Committee on Taxonomy of Viruses*”, *San Diego: Academic Press*., 2000, p. 657-678.**
5. **Lin, T.Y. et al. “*Enterovirus 71 outbreaks, Taiwan: occurrence and recognition*”, *Emerging Infectious Diseases*, 2003, 9(3): p. 291-293.**
6. **Wang, S.F. “*An epidemiological analysis of enterovirus 71: Taiwan, 1998-2004*”, *Taiwan Epidemiology Bulletin*, 2005, p. 125-153.**
7. **Wu, H.S. et al. “*Update on the Molecular Epidemiology of Human Enterovirus 71 in Taiwan Since 1998*”, *International Journal of Infectious Diseases*, 2008, Vol. 12 (Supplement 1).**
8. **Chang, L.Y. et al. “*Comparison of enterovirus 71 and coxsackie-virus A16 clinical illnesses during the Taiwan enterovirus epidemic, 1998*”, *The pediatric infectious disease journal*, 1999, 18(12): p. 1092-1096.**
9. 行政院衛生署疾病管制局 “*腸病毒感染併發重症臨床處理注意事項*”, **2010.**

10. 行政院衛生署疾病管制局 *“傳染病防治工作手冊-腸病毒感染併發重症”*, **2008.**

11. 行政院衛生署疾病管制局 *“腸病毒感染防治手冊”*, **2007.**

12. **Wu, Y. et al. “*Single-crystal metallic nanowires and metal/semiconductor nanowire heterostructures”, Nature,* 2004, 430(6995): p. 61-65.**

13. **Schmidt, N.J. et al. “*An apparently new enterovirus isolated from patients with disease of the central nervous system”, The journal of infectious disease,* 1974, 129(3): p. 304-309.**

14. **Deibel, R. et al. “*Isolation of a new enterovirus” Proceedings of the Society for Experimental Biology and Medicine,* 1975. 148(1): p. 203-207.**

15. **Blomberg, J. et al. “*New enterovirus type associated with epidemic of aseptic meningitis and-or hand, foot, and mouth disease” Lancet,* 1974, 13(2): p. 112.**

16. **Tagaya, I. and Tachibana, K. “*Epidemic of hand, foot and mouth disease in Japan, 1972-1973: difference in epidemiologic and virologic features from the previous one”, Japanese journal of medical science & biology,* 1975, 28(4): p. 231-234.**

17. **Gilbert, G.L. et al. “*Outbreak of enterovirus 71 infection in Victoria, Australia, with a high incidence of neurologic involvement”, Pediatric Infectious Disease Journal,* 1988, 7(7): p. 484-488.**

18. **Shindarov, L.M. et al. “*Epidemiological, clinical and pathomorphological characteristics of epidemic poliomyelitis-like disease caused by enterovirus 71”, Journal of Hygiene Epidemiology Microbiology and Immunology,* 1979, 23(3): p. 284-295.**

19. **Nagy, G. et al. "*Virological diagnosis of enterovirus type 71 infections: experiences gained during an epidemic of acute CNS diseases in Hungary in 1978*", *Archives of Virology*, 1982, 71(3): p. 217-227.**

20. **World Health Organization (WHO) "*Outbreak of hand, foot and mouth disease in Sarawak. Cluster of deaths among infants and young children*", *Weekly epidemiological record*, 1997, 72, p. 211-212.**

21. **Ho, M.T. et al. "*An epidemic of enterovirus 71 infection in Taiwan*", *New England Journal of Medicine*, 1999, 341(13): p. 929-935.**

22. **World Health Organization (WHO) "*Enterovirus - non polio*", 2002 [cited; Available from: http://www.who.int/mediacentre/factsheets/fs174/en/index.html .**

23. **Shih, S.R. et al. "*Genetic analysis of enterovirus 71 isolated from fatal and non-fatal cases of hand, foot and mouth disease during an epidemic in Taiwan, 1998*", *Virus Research*, 2000, 68(2): p. 127-136.**

24. **Rigonan, A.S. et al. "*Use of monoclonal antibodies to identify serotypes of enterovirus isolates*", *Journal of Clinical Microbiology*, 1998, 36(7): p. 1877-1881.**

25. **Manzara, S. et al. "*Molecular identification and typing of enteroviruses isolated from clinical specimens*", *Journal of Clinical Microbiology*, 2002, 40(12): p. 4554-4560.**

26. **Chen, T.C. et al. "*Combining multiplex reverse transcription-PCR and a diagnostic microarray to detect and differentiate enterovirus 71 and coxsackievirus A16*", *Journal of Clinical Microbiology*, 2006, 44(6): p. 2212-2219.**

27. **Yan, J.J. et al. "*Complete genome analysis of enterovirus 71 isolated***

***from an outbreak in Taiwan and rapid identification of enterovirus 71 and coxsackievirus A16 by RT-PCR", Journal of Medical Virology,* 2001, 65(2): p. 331-339.**

28. **Lipson, S.M. et al. "*Detection of precytopathic effect of enteroviruses in clinical specimens by centrifugation-enhanced antigen detection", Journal of Clinical Microbiology*, 2001, 39(8): p. 2755-2759.**

29. **Guney, C. et al. "*Laboratory diagnosis of enteroviral infections of the central nervous system by using a nested RT-polymerase chain reaction (PCR) assay", Diagnostic Microbiology and Infectious Disease*, 2003, 47(4): p. 557-562.**

30. **Wang, S.Y. et al. "*Early and rapid detection of enterovirus 71 infection by IgM-capture ELISA", Journal of Virological Methods*, 2004, 119(1): p. 37-43.**

31. **Lim, K.A. and Benyeshmelnick, M. "*Typing of viruses by combinations od antiserum pools- application to typing of enteroviruses (Coxsackie and Echo)", Journal of Immunology*, 1960, 84(3): p. 309-317.**

32. **Tsao, K.C. et al. "*Use of molecular assay in diagnosis of hand, foot and mouth disease caused by enterovirus 71 or coxsackievirus A 16", Journal of Virological Methods*, 2002, 102(1-2): p. 9-14.**

33. **Hu, J.T. et al. "*Controlled growth and electrical properties of heterojunctions of carbon nanotubes and silicon nanowires", Nature*, 1999, 399, p. 48-51.**

34. **Cui, Y. and Lieber, C.M. "*Functional nanoscale electronic devices assembled using silicon nanowire building blocks", Science*, 2001, 291(5505): p. 851-853.**

35. **Cui, Y. et al. "*Nanowire nanosensors for highly sensitive and selective detection of biological and chemical species*", *Science*, 2001, 293(5533): p. 1289-1292.**

36. **Hahm, J. and Lieber, C.M. "*Direct ultrasensitive electrical detection of DNA and DNA sequence variations using nanowire nanosensors*", *Nano Letters*, 2004, 4(1): p. 51-54.**

37. **Patolsky, F. et al. "*Electrical detection of single viruses*", *Proceedings of the National Academy of Sciences of the United States of America*, 2004, 101(39): p. 14017-14022.**

38. **Zheng, G.F. et al. "*Multiplexed electrical detection of cancer markers with nanowire sensor arrays*", *Nature Biotechnology*, 2005, 23(10): p. 1294-1301.**

39. **Patolsky, F. et al. "*Detection, stimulation, and inhibition of neuronal signals with high-density nanowire transistor arrays*", *Science*, 2006, 313(5790): p. 1100-1104.**

40. **Chen, Y. et al. "*Silicon-based nanoelectronic field-effect pH sensor with local gate control*" *Applied Physics Letters*, 2006, 89(22): p. 223512-223512-3.**

41. **Lud, S.Q. et al. "*Field effect of screened charges: Electrical detection of peptides and proteins by a thin-film resistor*", *Chemphyschem*, 2006, 7(2): p. 379-384.**

42. **Stern, E. et al. "*Label-free immunodetection with CMOS-compatible semiconducting nanowires*", *Nature*, 2007, 445(7127): p. 519-522.**

43. **Wong, S.S. et al. "*Covalently functionalized nanotubes as nanometre-sized probes in chemistry and biology*", *Nature*, 1998, 394(6688): p. 52-55.**

44. **Campagnolo, C. et al. *"Real-Time, label-free monitorine, of tumor antigen and serum antibody interactions", Journal of Biochemical and Biophysical Methods*, 2004, 61(3): p. 283-298.**

45. **Wu, G.H. et al. *"Bioassay of prostate-specific antigen (PSA) using microcantilevers", Nature Biotechnology*, 2001, 19(9): p. 856-860.**

46. **Ogi, H. et al. *"High-frequency wireless and electrodeless quartz crystal microbalance developed as immunosensor", Japanese Journal of Applied Physics Part 1-Regular Papers Brief Communications & Review Papers*, 2007, 46(7B): p. 4693-4697.**

47. **Michalet, X. et al. *"Quantum dots for live cells, in vivo imaging, and diagnostics", Science*, 2005, 307(5709): p. 538-544.**

48. **Zhang, Y.C. and Heller, A. *"Reduction of the nonspecific binding of a target antibody and of its enzyme-labeled detection probe enabling electrochemical immunoassay of an antibody through the 7 pg/mL-100 ng/mL (40fM-400pM) range", Analytical Chemistry*, 2005, 77(23): p. 7758-7762.**

49. **Shih, S.R. et al. *"Serotype-specific detection of enterovirus 71 in clinical specimens by DNA microchip array", Journal of Virological Methods*, 2003, 111(1): p. 55-60.**

50. **Hsiao, C.Y. et al. *"Novel poly-silicon nanowire field effect transistor for biosensing application", Biosensors & Bioelectronics*, 2009, p. 1223-1229.**

51. **Lin, H.C. et al. *"A simple and low-cost method to fabricate TFTs with poly-Si nanowire channel", IEEE Electron Device Letters*, 2005, 26(9): p. 643-645.**

52. **Su, C.J. et al. *"High-performance TFTs with Si nanowire channels***

***enhanced by metal-induced lateral crystallization", IEEE Electron Device Letters,* 2006, 27(7): p. 582-584.**

53. Lin, C.H. et al. "*Ultrasensitive detection of dopamine using a polysilicon nanowire field-effect transistor", Chemical Communications,* 2008, 44, p. 5749-5751.

54. Lin, H.C. et al. "*Water passivation effect on polycrystalline silicon nanowires", Applied Physics Letters,* 2007, 91(20): p. 202113.

55. Su, C.J. et al. "*Operations of poly-Si nanowire thin-film transistors with a multiple-gated configuration", Nanotechnology,* 2007, 18, p. 215205

56. Li, Z. et al. "*Sequence-specific label-free DNA sensors based on silicon nanowires", Nano Letters,* 2004, 4(2): p. 245-247.

57. Lin, C.H. et al. "*Poly-silicon nanowire field-effect transistor for ultrasensitive and label-free detection of pathogenic avian influenza DNA", Biosensors & Bioelectronics,* 2009, 24(10): p. 3019-3024.

58. Jensen, K.K. et al. "*Kinetics for hybridization of peptide nucleic acids (PNA) with DNA and RNA studied with the BIAcore technique", Biochemistry,* 1997, 36, p. 5072-5077.

59. Hook, F. et al. "*Characterization of PNA and DNA immobilization and subsequent hybridization with DNA using acoustic-shear-wave attenuation measurements", Langmuir,* 2001, 17, p. 8305-8312.

60. Hahm, J.I. and Lieber, C.M. "*Direct ultrasensitive electrical detection of DNA and DNA sequence variations using nanowire nanosensors", *Nano Letters,* **2004, 4(1), p. 51-54.**

Tables

Table 1

Enterovirus were classified based on their genomic sequences

Classified	Serotypes
Human enterovirus A (HEV-A)	Coxsackie virus A2-8, 10, 12, 14, 16
	Enterovirus 71, 76, 89-92
Human enterovirus B (HEV-B)	Coxsackie virus A9
	Coxsackie virus B1-6
	Echovirus 1-7, 9, 11-21, 24-27, 29-33
	Enterovirus 69, 73-75, 77-88, 93, 97-98, 100-101
Human enterovirus C (HEV-C)	Coxsackie virus A1, 11(15), 13(18), 17, 19-22, 24
	Enterovirus 95-96, 99, 102
	Poliovirus 1-3
Human enterovirus D (HEV-D)	Enterovirus 68, 70, 94
New (unclassified)	

Table 2

The common disease related enterovirus serotypes[11].

Common diseases	Virus serotype
hand-foot-mouth disease (HFMD)	Coxsackievirus group A16 (CA16), CA4, 5, 9, 10, CB2, 5, EV71
Herpangina	CA 1-10, CA16, CA22, EV71
Pleurodynia	Coxsackievirus group B (CB)
Acute myocarditis and pericarditis	CB
Acute meningitis and encephalitis	CA10
Aseptic meningitis and encephalitis	Coxsackievirus, poliovirus, echovirus, EV71
Febrile illness with rash	Coxsackievirus, echovirus

Table 3

Proposed pathogenesis of severe Enterovirus 71 infections [3]

Stage	Syndrome	Underlying cause
1	Hand-foot-and-mouth disease (HFMD)/ herpangina	-
2	Encephalomyelitis	Direct invasion or viremia
3	Cardiopulmonary failure A: Hypertension B: Hypotension	Neurogenic inflammatory response
4	Convalescence	-

Table 4

Historical perspective and case incidences of Enterovirus 71 in worldwide.

Year	Description
1969	First isolated in California
1972	Melbourne, Australia
1974	Sweden
1973	Japan
1975	Bulgaria with 44 deaths
1978	Hungary with 45 deaths
	Japan
1985	Hong Kong
1986	Nan-ao, Taiwan
1997	Malaysia with at least 30 deaths
1998	Taiwan with 78 deaths
2000	Taiwan with 25 deaths
2001	Taiwan with 26 deaths

Table 5

The detection limit of all kinds of novel sensors.

Transducers	Target	Sensitivity
SPR[44]	Tumor antigen	10-100 pg/ml
Microcantilever [45]	PSA	0.2 ng/ml
QCM[46]	Human-IgG	100 pg/ml
Electrode [48]	IgG	7 pg/ml
SNW-FET[38]	PSA	50-100 fg/ml

Table 6

Chip electrical conditions and rank classfication

	Best	Acceptable	Failed
conditions	1. I_D increase dramatically in small voltage change(< 2V) 2. I_D value On/Off ratio > 4~5 order 3. I_D/I_G > 3order 4. The I_D-V_G curve is repeatable 5. Device turn on current I_D~10^{-7}or10^{-6} 6. The threshold voltage is closed to 0V in linear scale plot	Doesn't reach the conditions of failed chip, but interior than the best chips in electrical properties.	1. I_D/I_G < 3order 2. I_D value On/Off ratio < 4 order 3. Device doesn't turn on until V_G over 3V 4. V_{on}-V_{off} > 3V 5. I_D turn on current <10^{-8}

Table 7

Comparison among nucleotide biosensors

Real-time measurements	Sensing targets	Detection Limit
SPR [58]	PNA-DNA or PNA-RNA	10 nM
QCM [59]	PNA-DNA or DNA-DNA	1 μM
Single Si NWFET [60]	PNA-DNA	10 fM
Poly Si NWFET	DNA-DNA	1~100 fM

Figures

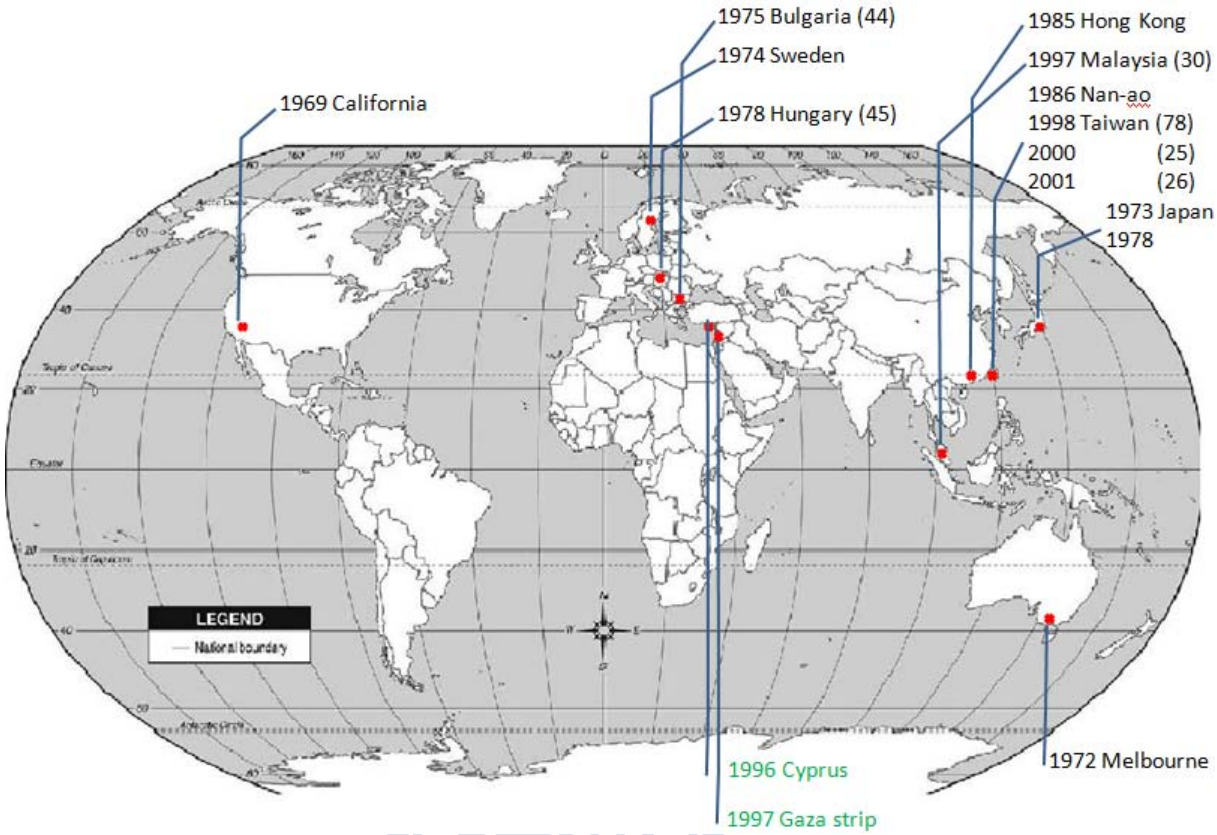

Figure 1 The epidemiology of enterovirus around the world, since 1969.

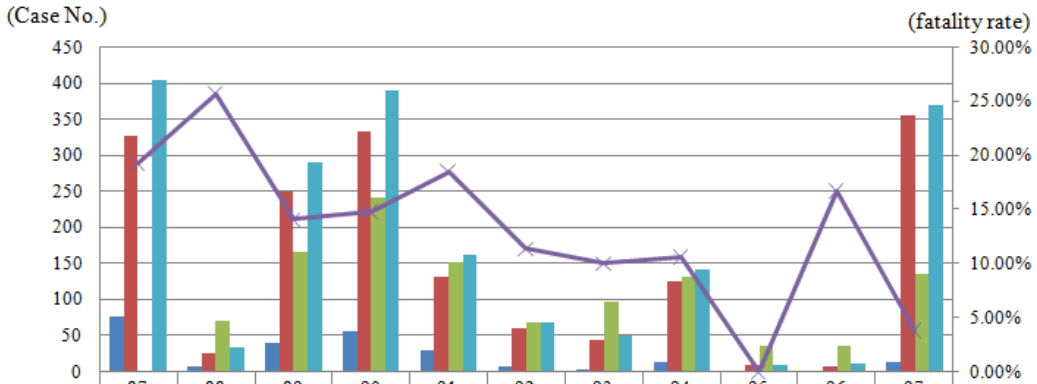

	87	88	89	90	91	92	93	94	95	96	97
Confirm fatal case No.	78	9	41	58	30	8	5	15	0	3	14
Confirm survival case No.	327	26	250	333	132	62	45	127	11	9	356
Exclude case No.	0	72	166	242	153	69	98	133	37	37	137
Total confirm case No.	405	35	291	391	162	70	50	142	11	12	370
Fatality rate	19.30%	25.70%	14.10%	14.80%	18.50%	11.40%	10%	10.60%	0%	16.70%	3.83%

Figure 2 Epidemic situation of Enterovirus infection with severe complications in Taiwan, 1998-2008. (redraw from CDC, 疫情報導 676, 938)

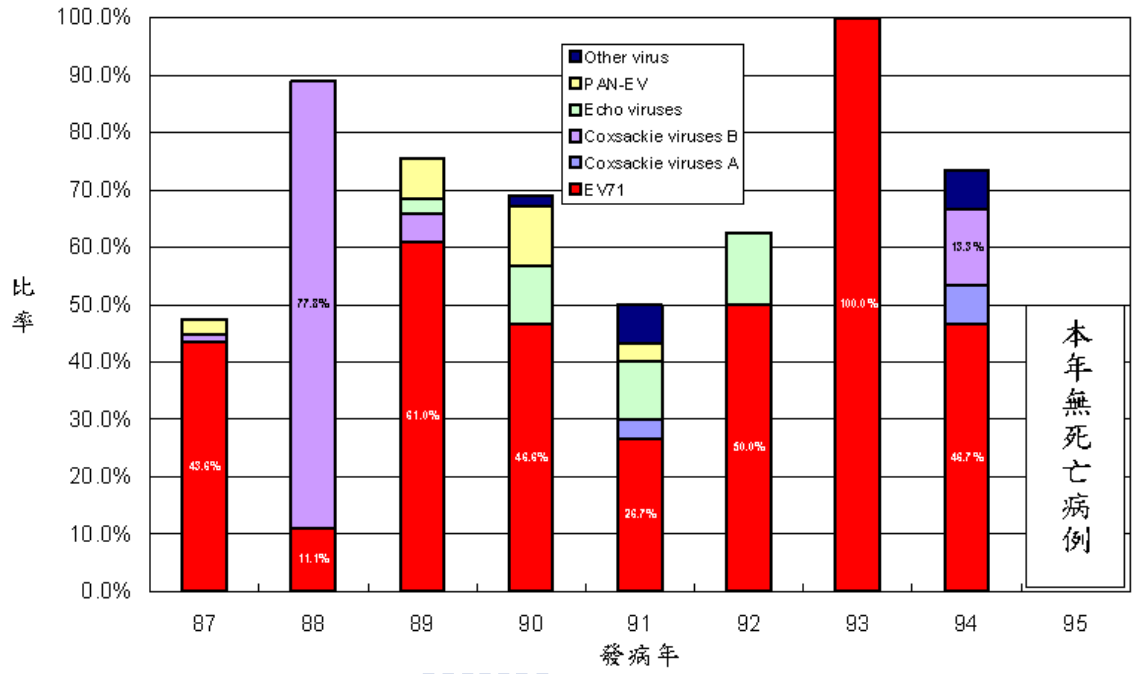

Figure 3 The distribution of serotypes of virus isolation from severe fatal case, 1998~2006 [11]

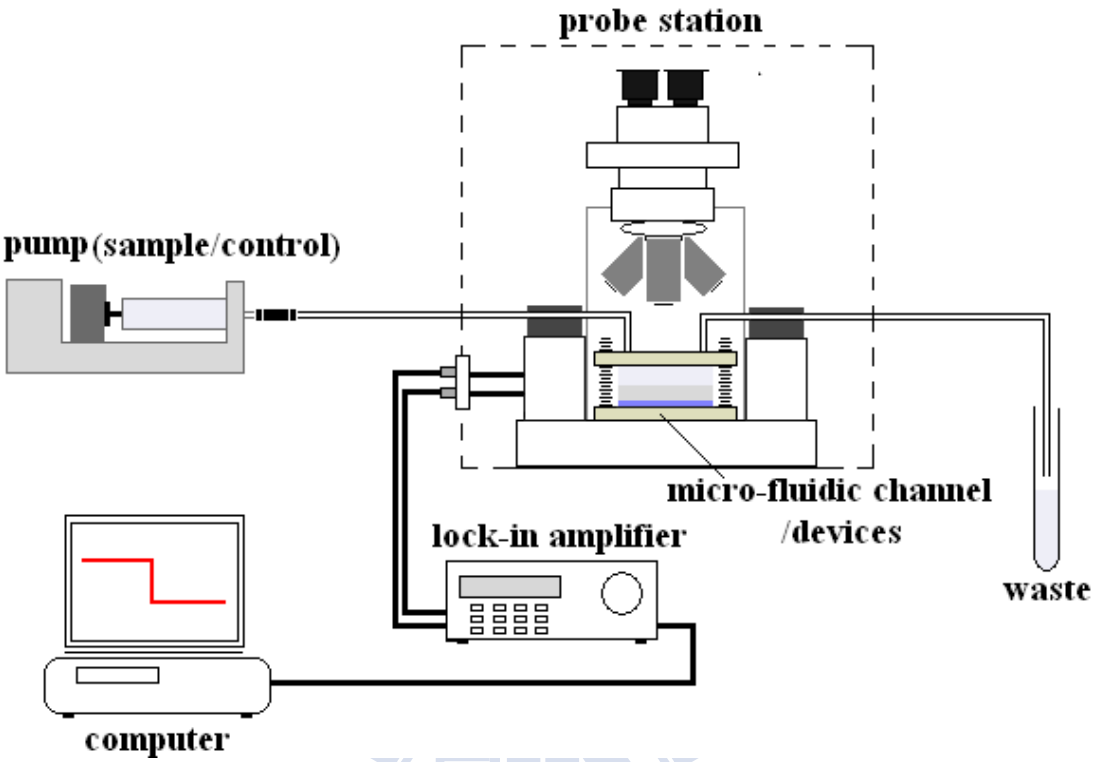

Figure 4 Overview of biosesing instruments.

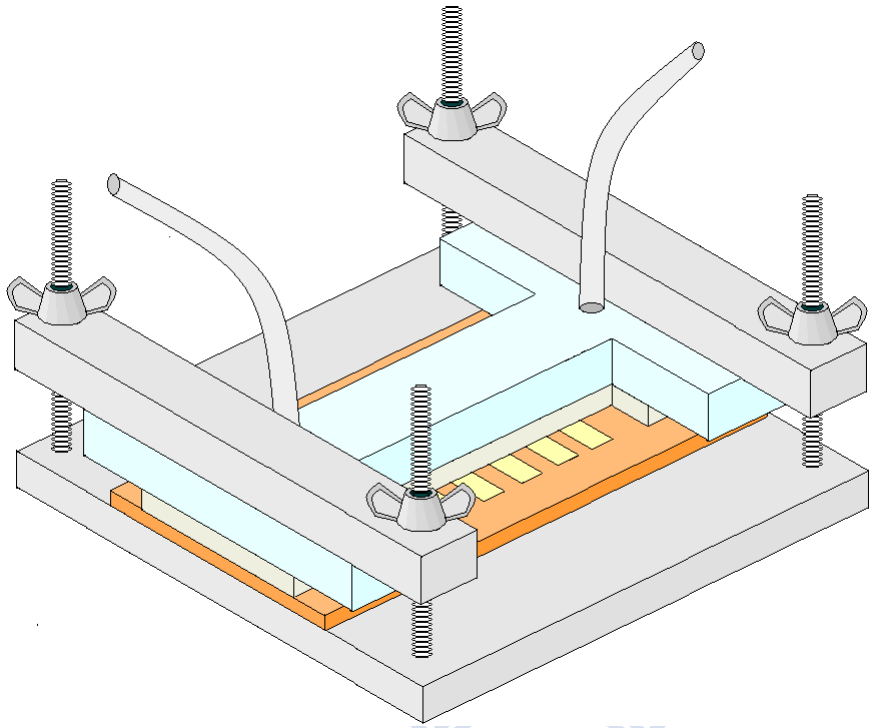

Figure 5 Schematic diagram of microfluidic channel for the biosensing with Si NW FET

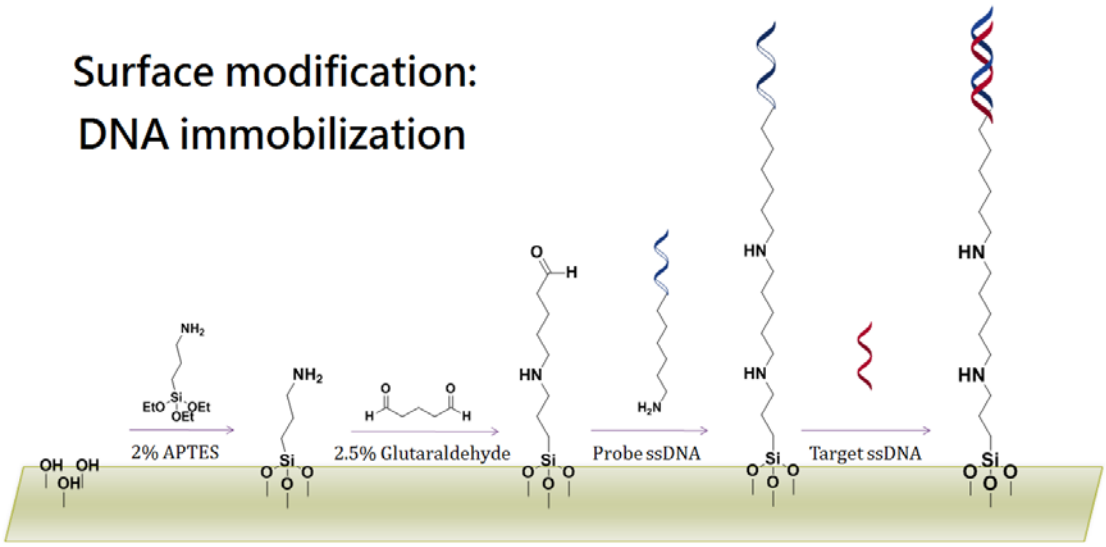

Figure 6 DNA immobilization process in microfluidic system

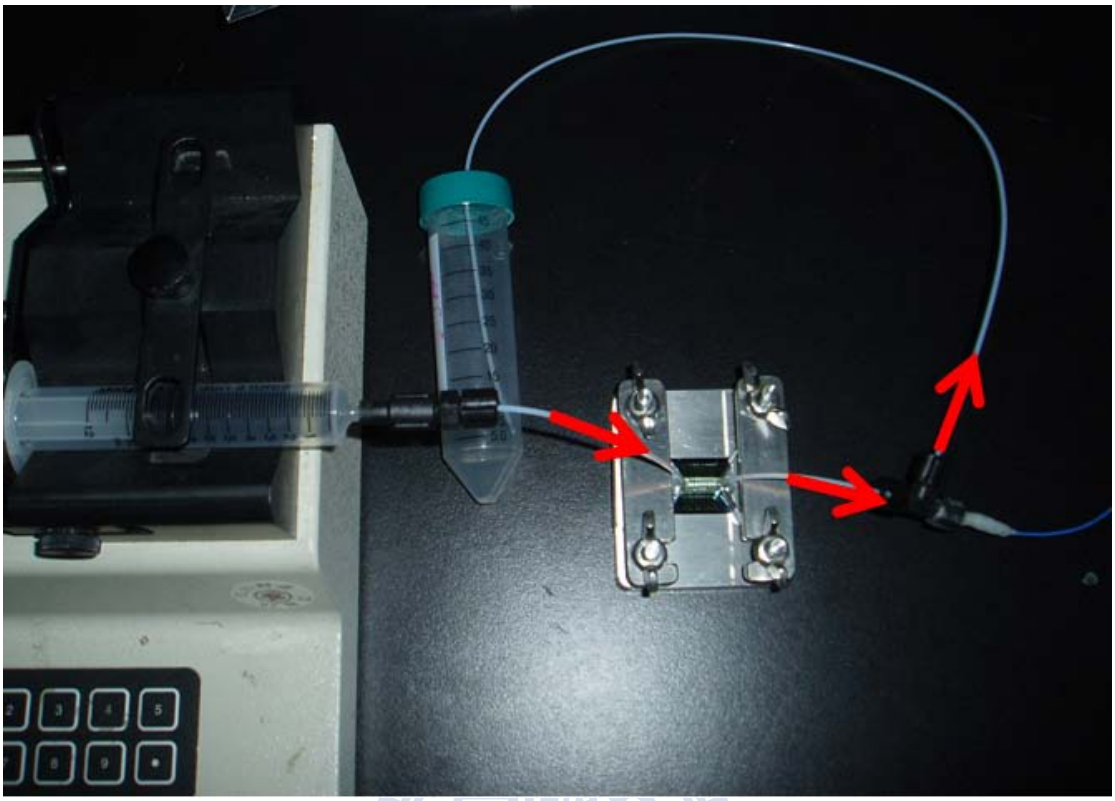

Figure 7 Sample transport direction and waste buffer bypass device

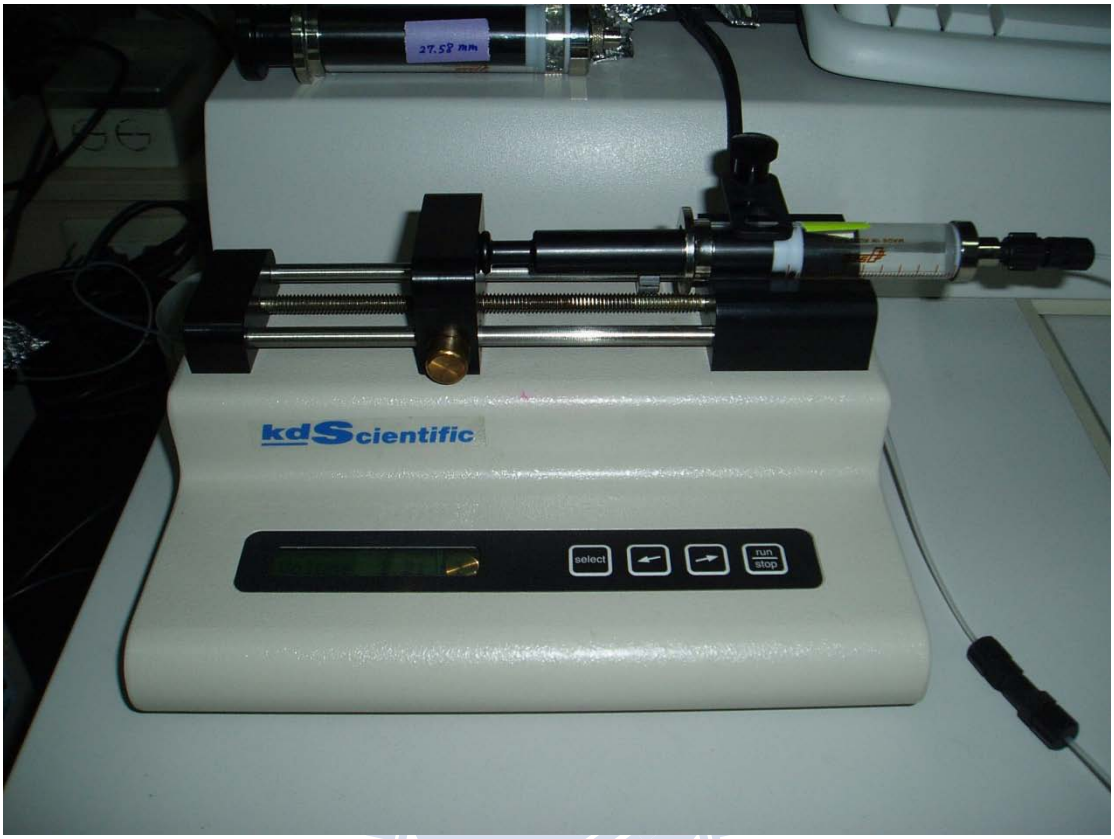

Figure 8 Programming Syringe pump (Fix the flow rate and volume by machine)

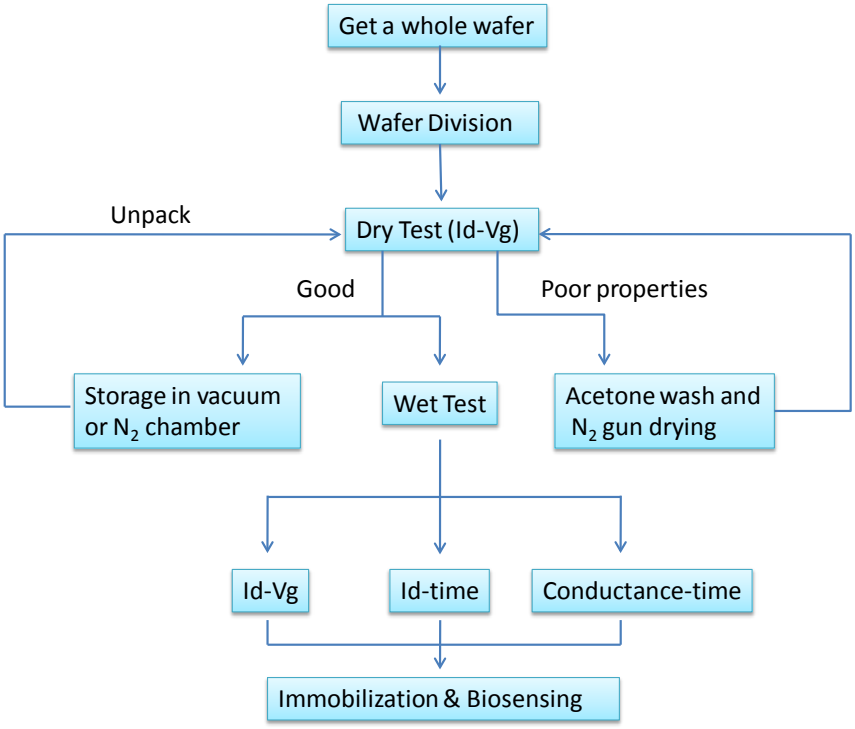

Figure 9 Standard operation process of device selection in dry air

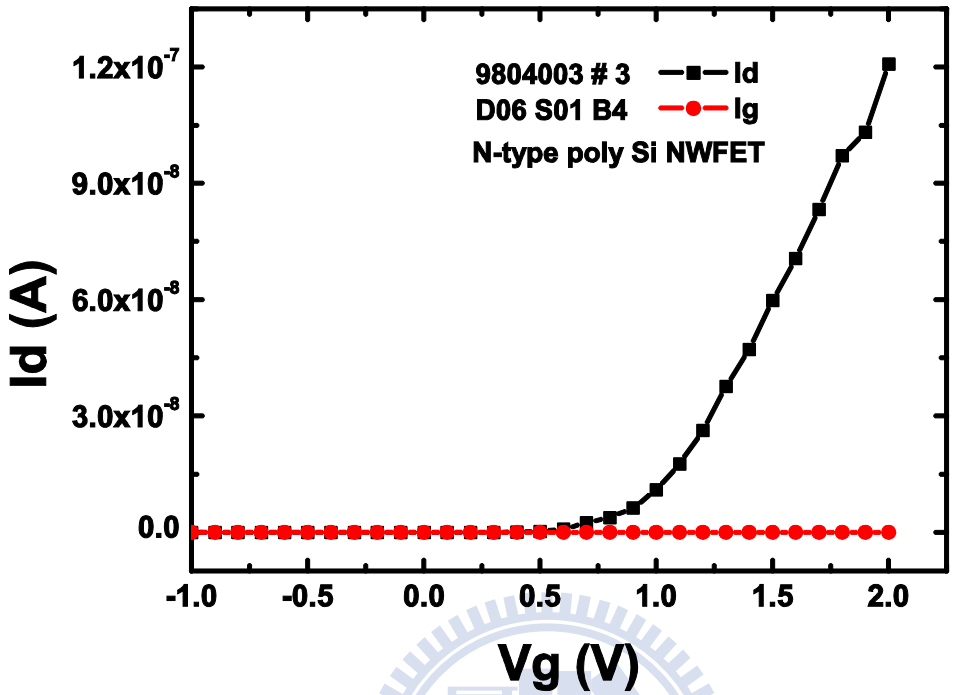

Figure 10-A N-type poly-Si NWFET measurement in dry air Vsd= 0.5V , Vgd sweep from -1V to 2V, threshold voltage ~ 1.0V .

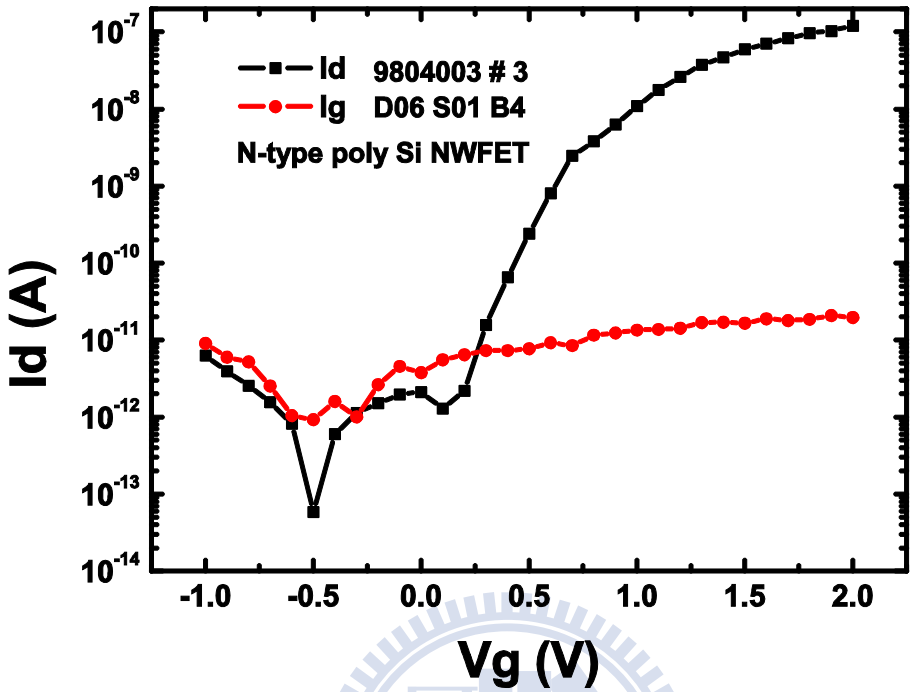

Figure 10-B The same data as Fig. 1A but in form of log scale plot. Its' drain current Id from 10^{-12} A to 10^{-7}A, leakage current Ig~10^{-12}A , on/off ratio~10^{5} .

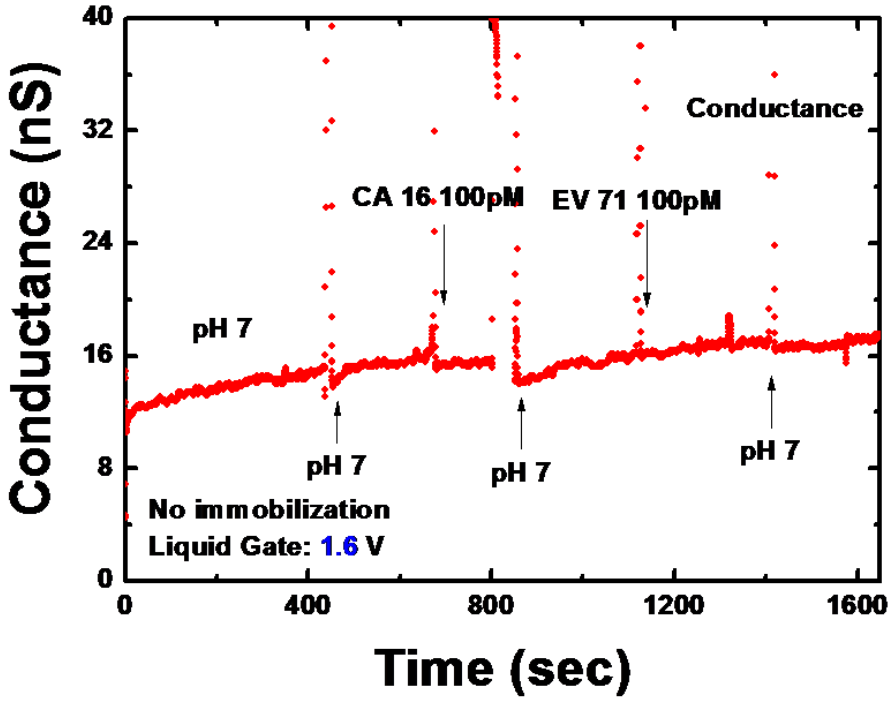

Figure 11 Without any immobilization process, this biosensing acts as a control set.

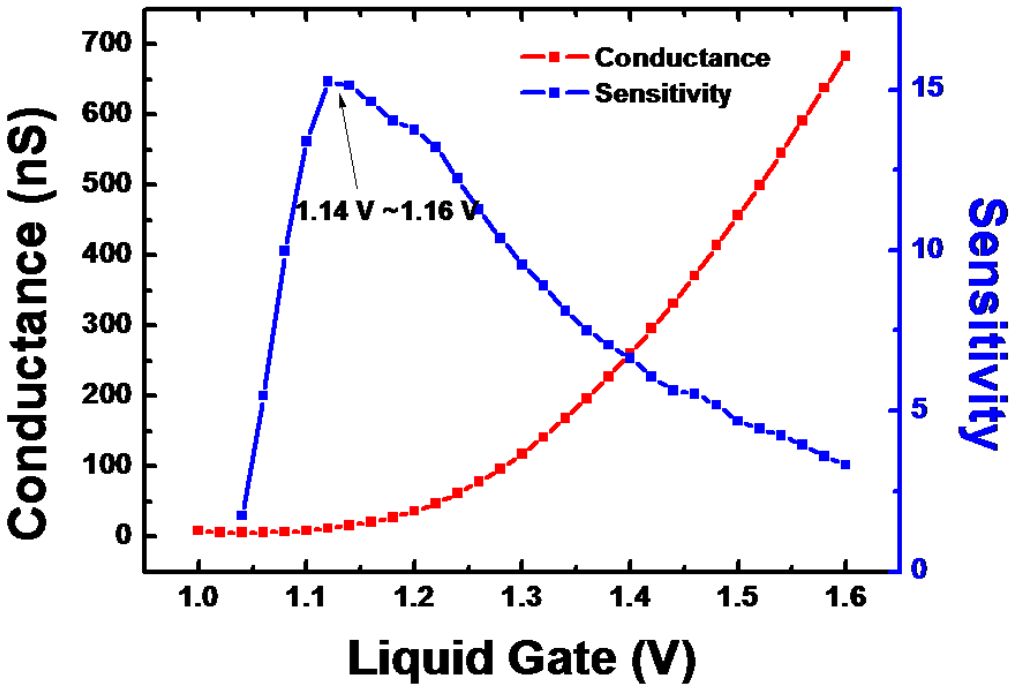

Figure 12 Conductance vs. Liquid gate plot accompany with the sensitivity variation trend.

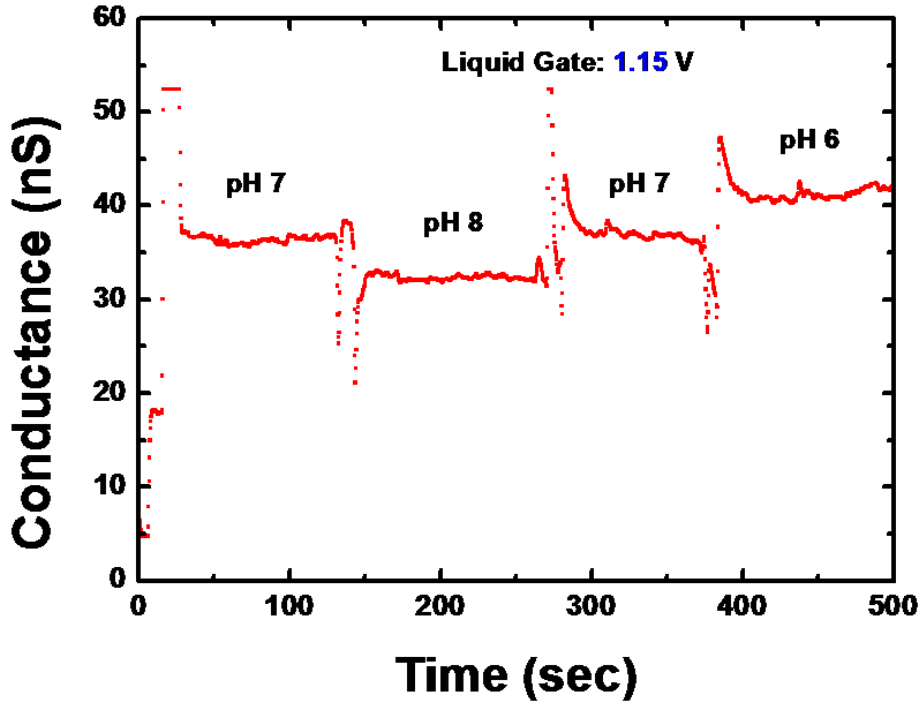

Figure 13 N-type NWFET pH sensing at fixed liquid gate (1.15V)

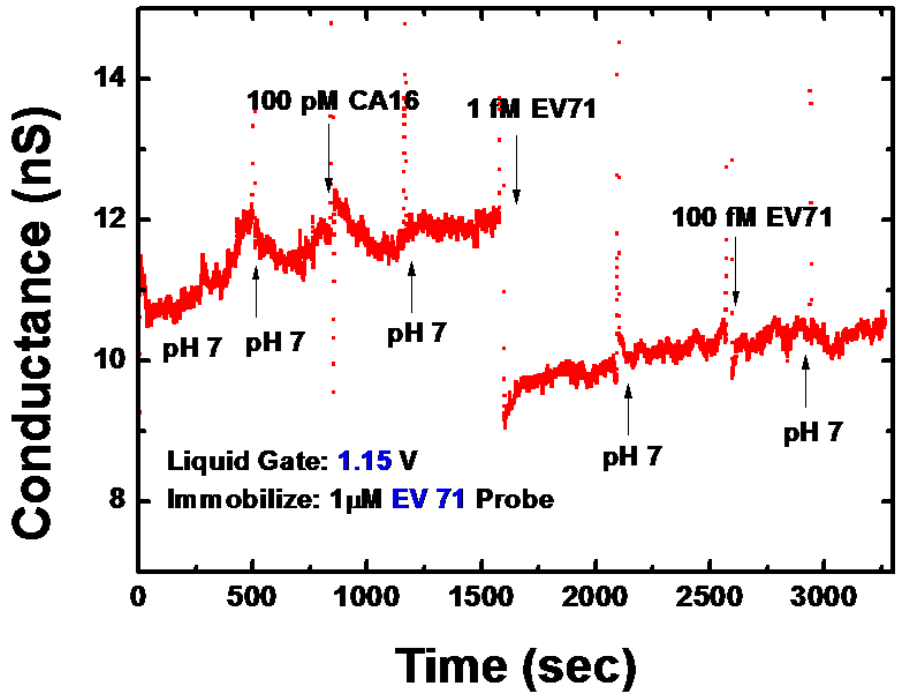

Figure 14 Real-time biosensing process of EV 71 (phosphate buffer elution between each sample in fixed flow rate: 5 ml/h).

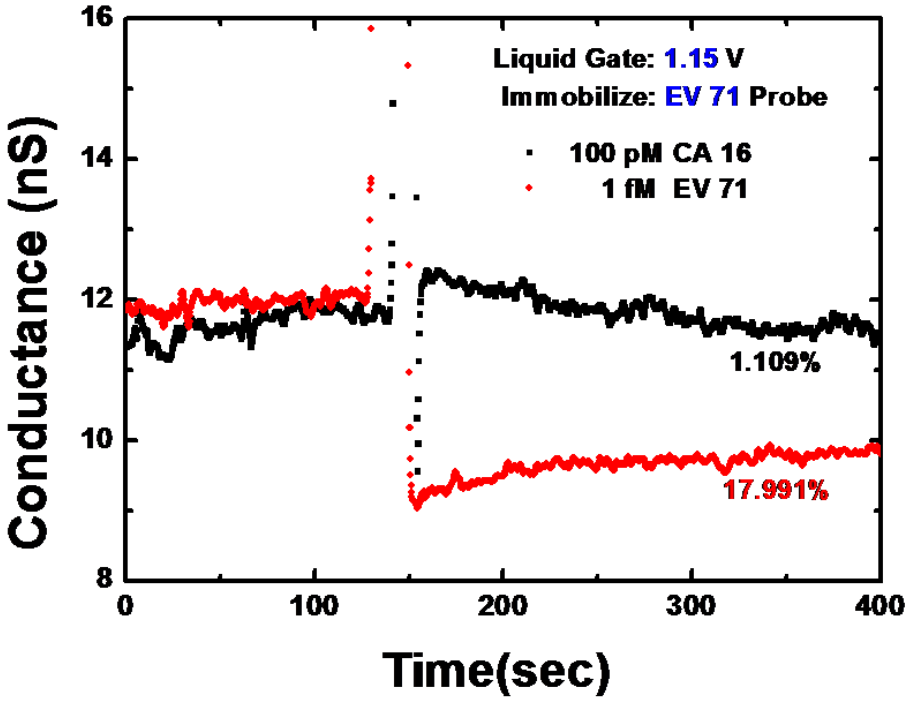

Figure 15 Compare the conductance variation rate between 10 pM CA 16 (negative control) and 1fM EV 71(experiment).

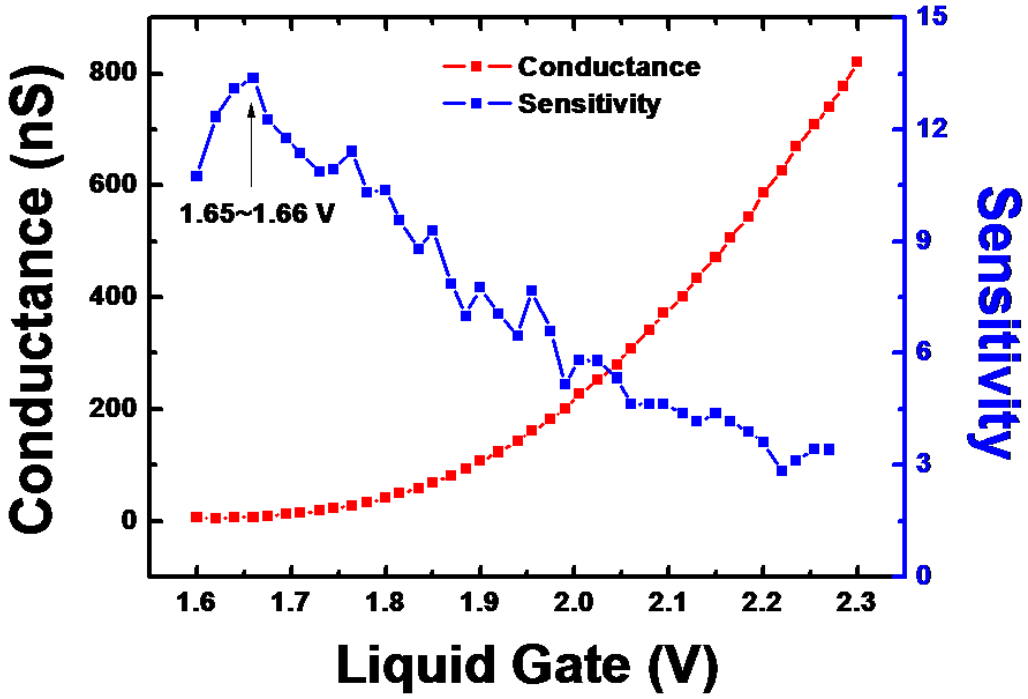

Figure 16 Conductance vs. Liquid gate plot accompany with the sensitivity factor after hot water washed

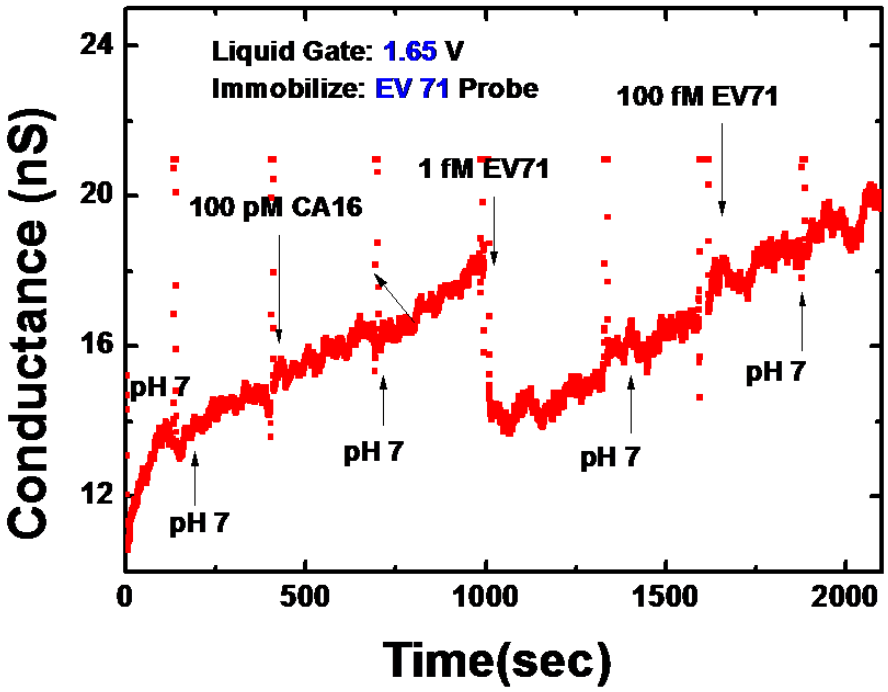

Figure 17 EV 71 biosensing process after hot water washed condition.

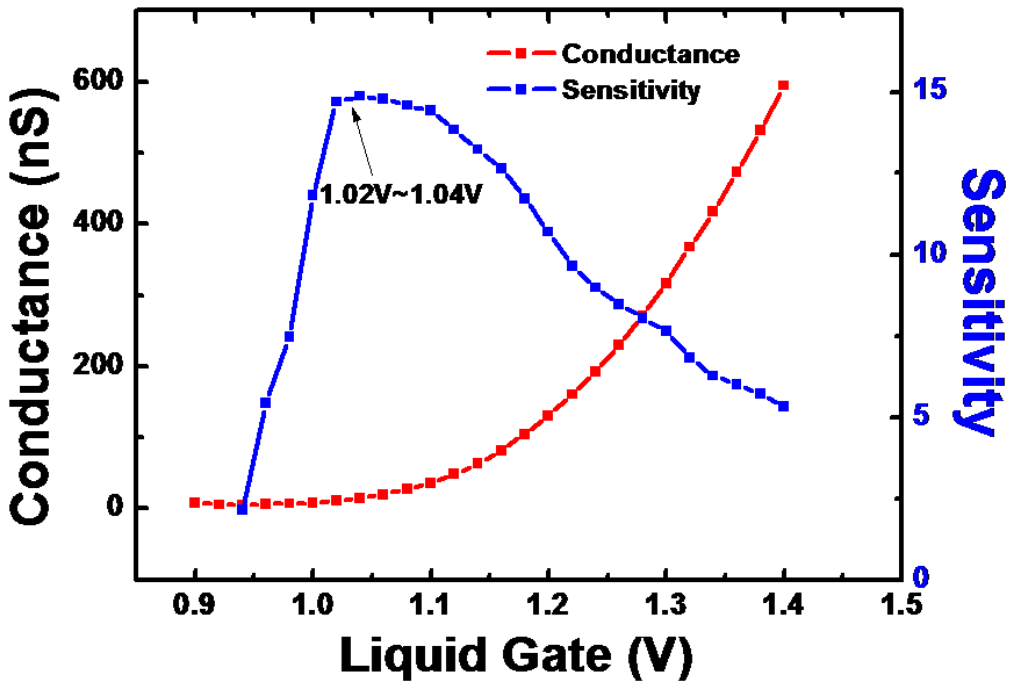

Figure 18 Calculating the most sensitive point of CA 16 biosensing

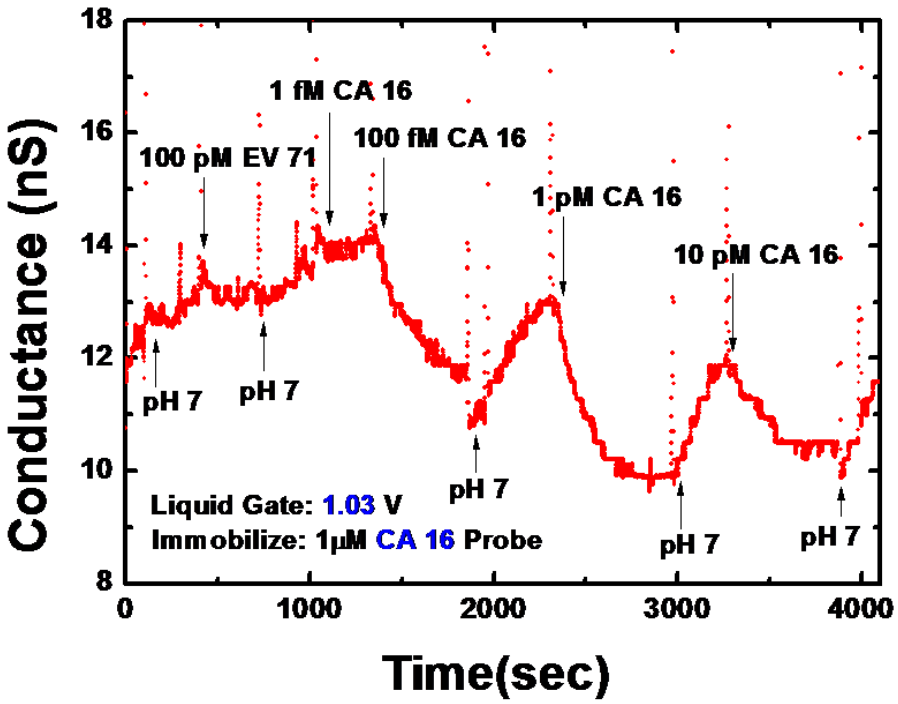

Figure 19 CA 16 Biosensing Process, the conductance value would reverse after pH 7 buffer solution flushed

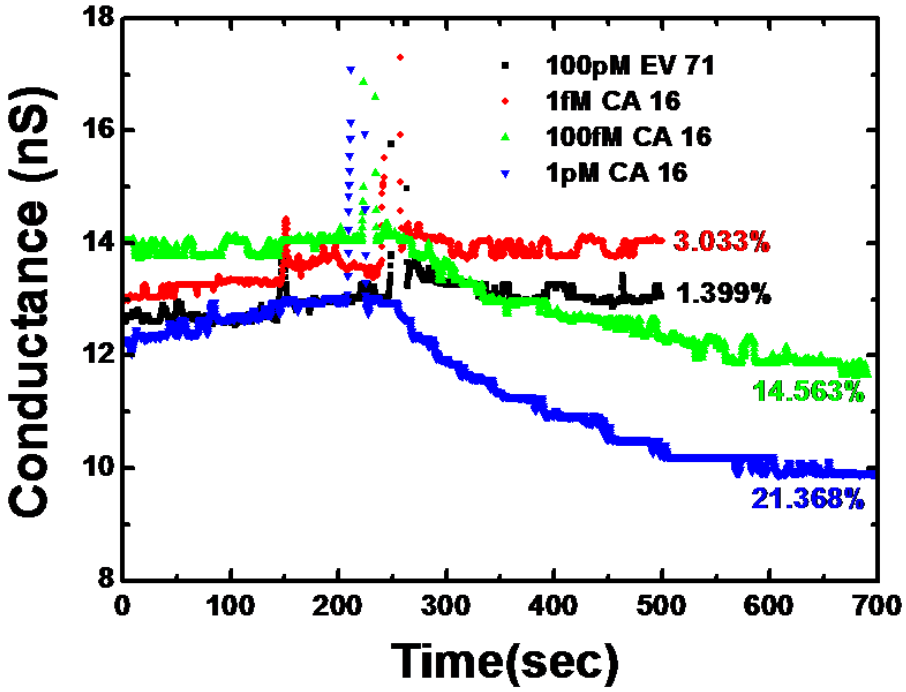

Figure 20 Comparison of different CA 16 DNA samples with control set